

# Kinetics of non-isothermal oxidation of anhydrous milk fat rich in conjugated linoleic acid using differential scanning calorimetry

Sergio I. Martínez-Monteaquedo ·  
Marleny D. A. Saldaña · John J. Kennelly

Received: 7 March 2011 / Accepted: 10 May 2011 / Published online: 26 May 2011  
© Akadémiai Kiadó, Budapest, Hungary 2011

**Abstract** Anhydrous milk fat (AMF) with low, medium, and high content of conjugated linoleic acid (L-, M-, and H-CLA) was oxidized using differential scanning calorimetry (DSC) at five different heating rates (3, 6, 9, 12, and 15 °C min<sup>-1</sup>) in a temperature range of 100–350 °C. For the first time, kinetic oxidation parameters of AMF rich in CLA are reported. DSC spectra were analyzed to locate the start temperature ( $T_s$ ), onset temperature ( $T_{on}$ ), and maximum heat flow temperature ( $T_p$ ). These reference points were further used to calculate the effective activation energy ( $E$ ) and pre-exponential factor ( $z$ ) using the Ozawa-Flynn-Wall method. The  $T_s$  shifts to lower values as the CLA content increases, while the  $T_{on}$  and  $T_p$  were less affected by the CLA content. The calculated kinetic parameters not only depend on the ratio between unsaturated to saturated fatty acids but also on the selected reference points. For the L-CLA sample, the  $E$  values calculated from  $T_s$ ,  $T_{on}$ , and  $T_p$  were 146.51, 114.11, and 121.31 kJ mol<sup>-1</sup>, respectively. For the M-CLA sample, the  $E$  values calculated were 112.42, 104.06, and 87.41 kJ mol<sup>-1</sup>, respectively. For the H-CLA sample, the  $E$  values calculated were 87.60, 82.42, and 73.64 kJ mol<sup>-1</sup>, respectively. These variations in  $E$  values do not have any physical background according to the compensation effect. In non-isothermal oxidation of AMF, several reactions with different kinetic parameters simultaneously take place and DSC only detects those reactions that have the highest

exothermal effect. The  $T_s$  is the most consistent reference point to calculate  $E$  and  $z$  values.

**Keywords** Anhydrous milk fat · Effective activation energy · Conjugated linoleic acid · DSC · Kinetic oxidation

## Introduction

The benchmark for any form of lipid-based product is the oxidative stability or resistance to oxidation [1]. Lipid oxidation is a free radical chain reaction that leads to the development of unpleasant taste and undesirable changes such as the formation of off-flavor compounds (aldehydes, ketones, etc.) [2]. Oxidation reactions consist of an initiation, a propagation and a termination stage. During the initiation stage, free radicals are formed through thermolysis and due to the presence of enzymes and active oxygen species. Then, these radicals react with molecular oxygen to form primary products such as hydroxiperoxides. These compounds are unstable and further react through free radical mechanisms to form secondary products that propagate the oxidation. The resulting compounds form viscous materials through polymerization as the oxidation proceeds. These polymers are oil insoluble and represent the termination stage of oxidation [3, 4].

Several methods have been used to analyze and monitor lipid oxidation [5]. These methods allow quantifying one or more reaction products of the different oxidation stages. Some of these methods are officially accepted by the American of Analytical Communities (AOAC) such as oxidative stability index (OSI) and peroxide values (PV) [5, 6], while others are routinely conducted, such methods are Rancimat, chemiluminescent, and volumetric methods. The oxidation process cannot be measured by a single test

S. I. Martínez-Monteaquedo · M. D. A. Saldaña (✉) ·  
J. J. Kennelly  
Department of Agricultural, Food and Nutritional Science,  
Faculty of Agricultural, Life and Environmental Sciences,  
University of Alberta, Edmonton, AB T6G 2P5, Canada  
e-mail: marleny@ualberta.ca

due to its complexity. As the oxidation proceeds, several reactions occur simultaneously at different rates. These reactions release heat that can be measured using differential scanning calorimetry (DSC). Recording the heat released from a particular reaction using DSC can be conducted in either isothermal or non-isothermal mode. In general, non-isothermal methods are widely used in lipid oxidation because they can provide valuable analytical and kinetic information. In addition, DSC method is simple, convenient, and fast [4, 7].

The non-isothermal method is based on the linear correlation between the temperature that corresponds to a specific thermal event and at a different heating rate [8]. From this relationship that follows an Arrhenius type equation, the effective activation energy ( $E$ ), pre-exponential factor ( $z$ ), and constant rate ( $k$ ) are derived. Kinetic information of lipid oxidation has been reported in soybean/anhydrous milk fat blends [9], natural unsaturated fatty acids (oleic, linoleic, and linolenic acids) [10], saturated fatty acids (lauric, myristic, palmitic, and stearic acids) [11], natural vegetable oils (canola, corn, cottonseed, and soybean oils), and genetically modified vegetable oils [4].

Anhydrous milk fat (AMF) is a versatile dairy ingredient with various applications in confectionary, bakery, and dairy products. It imparts hardness to confectionary products and it is used for the manufacture of lipid shortenings to structure or plastify vegetable oils. In addition, AMF is the major dietary source of conjugated linoleic acid (CLA) in human diet. CLA are positional and geometrical isomers of linoleic fatty acid, with a conjugated double-bond system [12]. Epidemiological studies have positively related CLA intake with health-promoting and disease-preventing properties [13]. Although these relationships are still under investigation, CLA has proven biological activity, including cancer prevention, atherosclerosis, weight control, and bone formation [14, 15]. CLA is naturally found in cow's milk (5 mg of CLA/g of fat). CLA concentration in AMF can be markedly enhanced through diet manipulation and nutritional management of dairy cows, as previously reported by Kennelly and Bell [16].

Searching alternatives to enhance AMF functionality by enrichment with CLA, certainly has health benefits and consequently commercial implications. However, CLA is susceptible to autoxidation upon thermal processing due to its conjugated double bond system ( $C=C$ ), which serves as an active site for free radical reactions. Kinetic data derived from Arrhenius type relationship such as the effective activation energy, pre-exponential factor and constant rate are essential parameters to predict oxidative stability. The non-isothermal oxidation kinetics of AMF enriched with CLA has not been reported so far. Therefore, the objective of this study was to evaluate the effect of CLA content on the non-isothermal oxidation kinetic of AMF.

## Materials and methods

### Anhydrous milk fat with different CLA concentrations

Three different feeding regimes were provided to dairy cattle at University of Alberta dairy farm following the methodology described by Kennelly and Bell [16, 17]. Then, anhydrous milk fat was obtained from CLA enriched milk, following the procedure described elsewhere [18] (Fig. 1). In brief, the raw milk was heated to 55 °C and centrifuged at 6000× $g$  for 6 min using an Alpha-Laval centrifuge (LAPX 202, Lundm Scania, Sweden). The cream obtained was stirred for 20 min at room temperature using a hand Black Decker Power Pro Mixer. The butter milk was discarded and the butter was washed with cold water to remove excess of butter oil. The butter was heated at 60 °C for 120 min until the different layers started to separate. Then, the top layer was removed and the mixture was poured through cheese cloth to obtain AMF. This fat was stored at −18 °C until further analysis.

### Fatty acids determination

Fatty acid profiles, including CLA were analyzed by gas-chromatography (GC) using the methodology described by Cruz-Hernandez et al. [19]. The GC (Varian 3400, Palo Alto, CA) instrument is equipped with a splitless injection port, a flame-ionization detector, an autosampler, and a

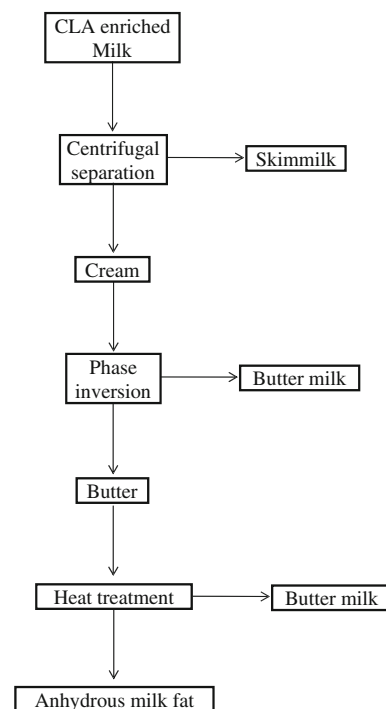


**Fig. 1** Schematic diagram of anhydrous milk fat production (Adapted from Walstra et al. [18])

100-m SP-2560 fused-silica capillary column (Supelco Inc., Bellefonte, PA). Base-catalyzed methylation was used to obtain fatty acid methyl esters (FAME). AMF rich in CLA (3 mg) was mixed with 2 mL of hexane, 40  $\mu\text{L}$  of methylacetate, and 80  $\mu\text{L}$  of sodium methoxide (0.5 N). The mixture was allowed to react for 20 min at 60  $^{\circ}\text{C}$ . After incubation time, hexane (2 mL), 2 mL of water and 1 mL of internal standard were added. The internal standard was prepared by dissolving 0.05 g of methyl heptadecanoate (C17:0, Fluka #51633 purity 99.5%, Sigma-Aldrich, Saint Louis, MO) in 50 mL of hexane. The upper phase of the solution that contained the FAME was transferred to GC vials and diluted with hexane (0.4 mg of FAME in 1 mL of hexane). Samples of 100  $\mu\text{L}$  of FAME solution were injected under a  $\text{N}_2$  flow rate of 1  $\text{mL min}^{-1}$ . The injector and detector temperature was 250  $^{\circ}\text{C}$ . The injected samples were heated at 45  $^{\circ}\text{C}$  for 4 min, then heated to 175  $^{\circ}\text{C}$  at 13  $^{\circ}\text{C min}^{-1}$  and held for 27 min, and then heated to 215  $^{\circ}\text{C}$  at 4  $^{\circ}\text{C min}^{-1}$  for 35 min [20]. The spectra were analyzed with Galaxi software version V1.19 and the peaks were identified by comparison with a GC milk fat reference FAME standard (463-Nu Check Prep Inc., Elysian, MN).

#### Differential scanning calorimetry determination

The oxidation kinetics of anhydrous milk fat samples was performed in a Q100 Modulated Differential Scanning Calorimeter (TA instruments, New Castle, DE). Samples of 1–2 mg were placed into aluminum pans with a pinhole lid (TA instruments, New Castle, DE) and were hermetically sealed. An empty sealed aluminum pan was used as a reference and the experiments were performed under an oxygen (dry 99% pure, Praxair, Edmonton, AB, Canada) flow rate of 50  $\text{mL min}^{-1}$  at 20 psi. These conditions allowed the interaction of the sample and the oxygen and were kept constant during the entire heating protocol. The sealed pans were equilibrated at 100  $^{\circ}\text{C}$  for 1 min and then heated to 350  $^{\circ}\text{C}$  at linear increased program rates (3, 6, 9, 12, and 15  $^{\circ}\text{C min}^{-1}$ ) to generate the oxidative profile (heat flow against temperature). The spectra were analyzed with a TA Universal Analysis software (TA instruments, New Castle, DE) to locate the start temperature ( $T_s$ ), onset temperature ( $T_{on}$ ), and maximum heat flow temperature ( $T_p$ ). They were precisely determined using the first and second derivatives of the signal (Fig. 2) [21].  $T_s$  is considered when the first derivative of the signal shows an inflexion point between a maximum and a minimum point of the signal (arrow 1) and the second derivative has reached a maximum point on the heat flow signal (arrow 2).  $T_p$  is considered when the first derivative of the signal intersects with the  $x$ -axis (arrow 3) and the second derivative has reached a maximum point on the signal (arrow 4).  $T_{on}$  was obtained extrapolating the tangent drawn on the

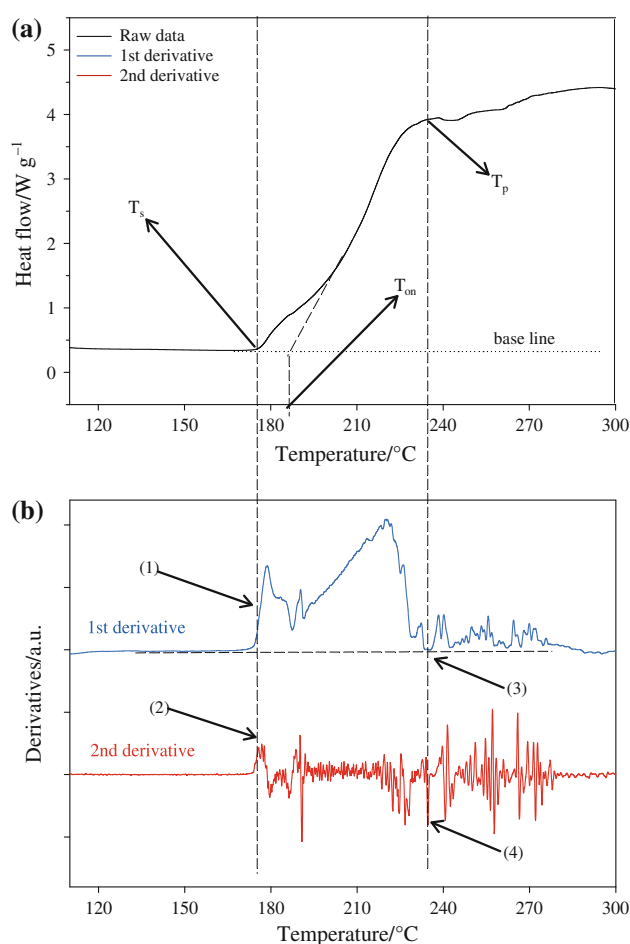


**Fig. 2** DSC oxidation curve of anhydrous milk fat with high CLA content at a rate of 15  $^{\circ}\text{C min}^{-1}$ . **a** Determination of start temperature ( $T_s$ ), onset temperature ( $T_{on}$ ) and maximum heat flow temperature ( $T_p$ ), and **b** zoom on the first and second derivatives that precisely locates the  $T_s$ ,  $T_{on}$ , and  $T_p$

steepest slope of  $T_p$ . All these values were further used to calculate the effective activation energy ( $E$ ) and the pre-exponential factor ( $z$ ) of the Ozawa-Flynn-Wall method. Using this method, a set of data ( $T_s$ ,  $T_{on}$ , and  $T_p$ ) was obtained for each heating rate ( $\beta = dT/dt$ ) from which the kinetic parameters were calculated as follows:

$$\log \beta = a \frac{1}{T} + b \quad (1)$$

where  $\beta$  is the heating rate (K/min) and  $T$  is the temperature  $T_s$ ,  $T_{on}$ , or  $T_p$  (K). By plotting  $\log \beta$  against  $1/T$ , the effective activation energy ( $E$ ) and the pre-exponential factor ( $z$ ) can be determined directly from the slope and intercept according to:

$$a = -0.4567 \frac{E}{R} \quad (2)$$

$$b = -2.315 + \log \left( z \frac{E}{R} \right) \quad (3)$$

where  $a$  and  $b$  are the slope and intercept from Eq. 1, respectively, and  $R$  is the universal gas constant ( $8.31 \text{ J mol}^{-1} \text{ K}^{-1}$ ). Therefore, the effective activation energy and constant rate ( $k$ ) are calculated from:

$$E = -2.19R \frac{d \log \beta}{dT^{-1}} \quad (4)$$

$$k = z \cdot \exp\left(\frac{-E}{RT}\right) \quad (5)$$

#### Degree of conversion

All kinetic parameters were calculated using the iso-conversional method proposed by Ozawa-Flynn-Wall in which a constant degree of conversion ( $\alpha$ ) was used for each point of interest in the DSC spectra ( $T_s$ ,  $T_{on}$ , and  $T_p$ ) based on the initial ( $\text{signal}_o$ ) and final ( $\text{signal}_f$ ) heat flow signals. The degree of the non-isothermal oxidation of AMF conversion was calculated as follows:

$$\alpha = \frac{\text{Signal}_o - \text{Signal}}{\text{Signal}_o - \text{Signal}_f} \quad 0 \leq \alpha \leq 1 \quad (6)$$

#### Statistical analysis

All data were collected at least in duplicates and are reported as mean values and standard deviations. The statistical analysis was conducted using the Sigmaplot software V11 for windows (SPSS Inc., Chicago, IL, USA). Turkey test was also performed ( $P < 0.05$ ).

## Results and discussion

#### Fatty acid analysis

Table 1 shows the composition of the major fatty acids of the three different AMF samples obtained as described earlier. Overall, AMF saturated fatty acids in high concentration were myristic (C14:0), palmitic (C16:0), and stearic (C18:0) acids. The concentration of these major fatty acids was within the range reported earlier by Jensen [22], whom compiled investigations on bovine milk fat from year 1995 to 2000. Important variations were observed in the ratio of unsaturated to saturated fatty acids between feeding regimes and, consequently, the amount of CLA is also significantly different as reported and explained by Bell et al. [17]. These authors used the biohydrogenation theory to explain the increment in the CLA content and therefore the changes in the ratio of unsaturated to saturated fatty acids. Importantly, using these feeding regimes, cow milk with different concentrations of CLA were obtained (Table 1), from which AMF was separated (Fig. 1) and used in the oxidation studies.

**Table 1** Fatty acid composition (% of total fatty acids) of low, medium, and high CLA AMF

Fatty acid <sup>a</sup>	L-CLA	M-CLA	H-CLA
C4:0	0.30 ± 0.09	0.28 ± 0.01	0.20 ± 0.02
C6:0	1.37 ± 0.01	1.41 ± 0.01	0.85 ± 0.02
C8:0	0.91 ± 0.01	0.88 ± 0.08	0.50 ± 0.01
C10:0	2.04 ± 0.03	2.17 ± 0.04	1.09 ± 0.01
C12:0	2.47 ± 0.04	2.48 ± 0.16	1.47 ± 0.01
C14:0	8.87 ± 0.16	8.87 ± 0.16	6.83 ± 0.06
C15:0	1.05 ± 0.01	0.93 ± 0.08	0.79 ± 0.01
C16:0	23.94 ± 0.23	19.11 ± 0.18	17.92 ± 0.01
C16:1 <i>t</i>	0.33 ± 0.01	0.41 ± 0.02	0.73 ± 0.01
C16:1 <i>c</i>	1.81 ± 0.13	1.09 ± 0.06	1.31 ± 0.01
C18:0	9.18 ± 0.13	13.02 ± 0.22	8.69 ± 0.25
C18:1 <i>t11</i>	1.89 ± 0.06	3.97 ± 0.07	11.06 ± 0.27
C18:1 <i>n7</i>	21.99 ± 0.11	21.66 ± 0.78	21.73 ± 0.45
C18:2	1.94 ± 0.01	2.35 ± 0.02	2.27 ± 0.02
C20:0	0.142 ± 0.01	0.13 ± 0.01	0.10 ± 0.01
CLA	0.73 ± 0.01	0.91 ± 0.01	3.23 ± 0.01
Ratio Uns/sat	0.71	0.86	1.36

Mean ± standard deviation based on duplicates

<sup>a</sup> *t* trans fatty acids, and *c* cis fatty acids

*L-CLA* anhydrous milk fat with low CLA content, *H-CLA* anhydrous milk fat with high CLA content, *M-CLA* anhydrous milk fat with medium CLA content

#### Oxidative profile

Figure 3 shows the DSC thermograms of anhydrous milk fat obtained at five heating rates (3, 6, 9, 12, and  $15 \text{ }^\circ\text{C min}^{-1}$ ) in the range of 100–350  $^\circ\text{C}$ . As the heating rate increases, the  $T_s$ ,  $T_{on}$ , and  $T_p$  temperatures increase. This behavior was similar for the three AMF samples (Fig. 3a–c). During slow heating, primary oxidation products such as hydroperoxides generated during the initial oxidation stage react with excess of oxygen to form low molecular weight compounds (intermediate oxidation products) such as aldehydes and acids that remain in solution, accelerating the degradation process. At fast heating rates, on the other hand, these intermediate products are lost through evaporation before they further react with the oil solution, shifting to high values the threshold DSC signal [4].

An additional experimental run that consisted of anhydrous milk fat heated at  $3 \text{ }^\circ\text{C min}^{-1}$  under nitrogen flow rate revealed that neither significant exothermal nor endothermal event was observed (bottom line in Fig. 3a–c). This suggests that melting, decomposition, and polymerization did not occur within the range of 100–350  $^\circ\text{C}$ . Similar findings were reported by Ulksowski et al. [23], whom analyzed the weight lost of lecithin during heating

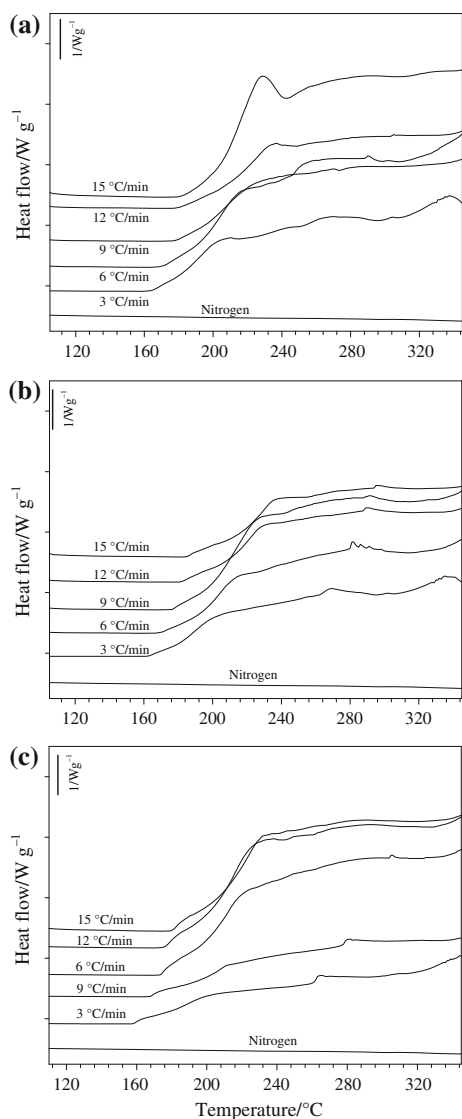


**Fig. 3** DSC oxidative profiles of anhydrous milk fat with low CLA content (a), medium CLA content (b), and high CLA content (c)

under nitrogen flow rate. Their thermogravimetric analysis showed that in the temperature range of 100–250 °C, only 4% of weight was lost but above 250 °C, the weight lost considerably increased. Therefore, changes in the DSC signal within the range of 100–250 °C were attributed to oxidation and those changes above 250 °C corresponded to thermal degradation rather than oxidation.

Table 2 summarizes the  $T_s$ ,  $T_{on}$ , and  $T_p$  temperatures of oxidation as a function of the heating rates. Comparing L-CLA versus H-CLA, the start, onset and maximum heat flow temperature shifts to lower values as the CLA content increases ( $P < 0.05$ ), mainly at low heating rates (3–9 °C min<sup>-1</sup>). This behavior can be a result of the different fatty acid composition of the three AMF samples (Table 1) and the fact that unsaturated fatty acids oxidize faster at low temperatures compared to saturated fatty acids

**Table 2** Start, onset and maximum heat flow temperatures of anhydrous milk fat oxidation obtained from DSC spectra at different heating rates ( $\beta$ )

$\beta/^\circ\text{C}/\text{min}$	Low CLA AMF	Medium CLA AMF	High CLA AMF
Start temperature of oxidation			
3	164.46 ± 0.09aA	161.91 ± 1.18abA	155.74 ± 3.44bA
6	177.57 ± 1.64aBD	170.39 ± 0.94abC	164.05 ± 5.63bC
9	175.52 ± 0.11aD	176.19 ± 0.30abD	170.95 ± 3.76bBC
12	173.52 ± 0.11aC	180.54 ± 2.41bcB	174.95 ± 1.69cBC
15	179.80 ± 0.84aB	184.04 ± 1.37abB	177.93 ± 3.40bB
Onset temperature of oxidation			
3	172.71 ± 0.20aA	173.47 ± 0.07abA	163.29 ± 1.62bA
6	184.01 ± 3.31aCE	184.71 ± 2.33aC	170.54 ± 0.85bC
9	183.16 ± 3.57aDE	192.13 ± 0.72abD	180.29 ± 3.35bD
12	187.32 ± 3.57aE	197.85 ± 3.71cB	188.50 ± 0.09bCE
15	195.07 ± 2.95aB	198.66 ± 0.39abB	191.97 ± 0.14bB
Maximum heat flow temperature of oxidation			
3	208.70 ± 1.47aA	212.67 ± 2.28aA	202.88 ± 1.27bA
6	221.14 ± 7.42aB	223.76 ± 0.85aC	211.20 ± 0.21bC
9	229.21 ± 5.98aB	236.62 ± 1.07abD	226.40 ± 2.82bD
12	231.43 ± 3.57aB	248.10 ± 16.07aBD	237.69 ± 0.85aB
15	229.94 ± 0.38aB	247.82 ± 3.63cB	239.50 ± 2.99bB

Mean ± standard deviation ( $n = 3$ ) within each row with different letters (a–c) are significantly different ( $P < 0.05$ ). AMF Anhydrous milk fat. Mean ± standard deviation within each column with different letters (A–E) are significantly different ( $P < 0.05$ )

which are detected by DSC signal. This behavior has been exemplified by non-isothermal oxidation of natural unsaturated fatty acids (oleic, erucic, linoleic, and linolenic acids [10]) and saturated fatty acids (lauric, myristic, palmitic, and stearic acids [24]). A decreasing tendency of start temperature of oxidation was observed with increasing the number of double bonds. For unsaturated compounds, the oxidation starts at lower temperatures due to C=C, which serves as an active site for free radical reactions such as autoxidation. Thus, in non-isothermal oxidation, the  $T_s$  values can be interpreted as formation of peroxide (autoxidation). An investigation of non-isothermal oxidized corn oil, linseed oil, and oleic acid at different known concentrations of peroxides showed that only  $T_s$  was affected by the initial presence of peroxide, while  $T_p$  was not affected [10]. Other investigations of oxidized linolenic acid in the presence of different phenolic compounds showed that the oxidative stability, measured by  $T_s$ , increases with increasing the concentration of antioxidant [2, 26].

#### Kinetic parameters

In DSC methods that are based on the recording of released heat in either isothermal or non-isothermal mode,



**Table 3** Kinetic and statistical parameters calculated from start, onset, and maximum heat flow temperatures

Sample	Parameters of Eq. 1		$R^2$	$E/\text{kJ mol}^{-1}$	$z/\text{min}^{-1}$	$k/\text{min}^{-1}$
	$a$	$b$				
Start temperature of oxidation, $T_s$						
L-CLA	-8046.2	18.91	0.955	146.51	$4.0 \times 10^{14}$	0.026
M-CLA	-6173.9	14.68	0.983	112.42	$3.6 \times 10^{10}$	0.014
H-CLA	-4810.8	11.82	0.964	87.60	$6.3 \times 10^7$	0.013
Onset temperature of oxidation, $T_{on}$						
L-CLA	-6267.1	14.57	0.974	114.11	$4.8 \times 10^{11}$	0.121
M-CLA	-5714.9	13.26	0.986	104.06	$2.0 \times 10^{10}$	0.065
H-CLA	-4531.2	10.92	0.947	82.42	$8.7 \times 10^7$	0.069
Maximum heat flow temperature, $T_p$						
L-CLA	-6662.1	14.31	0.981	121.31	$3.5 \times 10^{11}$	0.014
M-CLA	-4800.4	10.39	0.951	87.41	$3.0 \times 10^7$	0.006
H-CLA	-4044.1	9.02	0.943	73.64	$1.2 \times 10^6$	0.008

*L-CLA* anhydrous milk fat with low CLA content, *H-CLA* anhydrous milk fat with high CLA content, *M-CLA* anhydrous milk fat with medium CLA content,  $E$  effective activation energy,  $z$  pre-exponential factor,  $k$  constant reaction rate calculated at 200 °C (473 K),  $R^2$  regression coefficient,  $a$  and  $b$  coefficient parameters

the consumption of oxygen can be neglected due to the large excess of oxygen generated by a constant flow rate. Such condition allows the formation of peroxide being independently of the oxygen concentration, which also means that the autoxidation is a first order reaction [4, 22, 26]. This is an essential assumption for the calculation of kinetic parameters such as effective activation energy ( $E$ ), pre-exponential factor ( $z$ ), and reaction rate ( $k$ ). Using the information presented in Table 2 and according to Eqs. 1–4, the kinetic parameters were calculated and the values are presented in Table 3. According to Adhvaryu et al. [4], less than 1.5 mg of sample in a hermetically sealed pan with a pinhole provides consistent result. These recommendations were followed in the present study. For the L-CLA samples, the values of effective activation energy, calculated from  $T_s$ ,  $T_{on}$ , and  $T_p$ , were 146.51, 114.11, and 121.31  $\text{kJ mol}^{-1}$ , respectively. For the M-CLA samples, the  $E$  values were 112.42 ( $T_s$ ), 104.06 ( $T_{on}$ ), and 87.41 ( $T_p$ )  $\text{kJ mol}^{-1}$ , respectively. For the H-CLA samples, the  $E$  values were 87.60 ( $T_s$ ), 82.42 ( $T_{on}$ ), and 73.64 ( $T_p$ )  $\text{kJ mol}^{-1}$ , respectively. The  $k$  values from  $T_s$ ,  $T_{on}$ , and  $T_p$  calculated at 200 °C are shown in Table 3. For L-CLA samples, the  $k$  values calculated were 0.026 ( $T_s$ ), 0.121 ( $T_{on}$ ), and  $0.014 \text{ min}^{-1}$  ( $T_p$ ). For M-CLA samples, the values of  $k$  were 0.014 ( $T_s$ ), 0.065 ( $T_{on}$ ), and  $0.006 \text{ min}^{-1}$  ( $T_p$ ). For H-CLA samples, the  $k$  values were 0.013 ( $T_s$ ), 0.069 ( $T_{on}$ ), and  $0.008 \text{ min}^{-1}$  ( $T_p$ ). These variations can be attributed to differences in the ratio of unsaturated to saturated fatty acids. Thurgood et al. [9] studied the

non-isothermal oxidation of AMF and reported different activation energy values (93.56 and 57.55  $\text{kJ mol}^{-1}$ ) from onset and maxima heat flow temperatures, respectively. They also calculated the constant rate values at 200 °C (0.57 and  $0.10 \text{ min}^{-1}$ ) from onset and maxima heat flow temperatures, respectively. In addition, these authors also evaluated the non-isothermal oxidation of soybean/AMF blends. Again, the differences observed can be attributed to the ratio between unsaturated and saturated fatty acids. The authors generated the DSC curves using excess of AMF (6.5 mg) in an open aluminum pan, a procedure that might increase the thickness of the samples and, consequently, the diffusion of oxygen might be affected, influencing the results.

Table 3 shows that  $E$  values decrease as the amount of CLA content increases, regardless the selected reference point ( $T_s$ ,  $T_{on}$ , and  $T_p$ ). This behavior might be due to the oxidation of unsaturated fatty acids which started at low temperatures. But, values of  $E$  should not be considered as the only parameter to compare the non-isothermal oxidation of different lipid systems [9]. The constant reaction rate ( $k$ ) should also reflect the drop in the  $E$  values caused by the CLA content. In Table 3, the  $k$  values calculated at 200 °C from  $T_s$  decreased as the concentration of CLA increased. But,  $k$  values calculated from  $T_{on}$  and  $T_p$  do not exhibit the same pattern than those values calculated from  $T_s$ . This suggests that the start temperature of oxidation is the most consistent reference point in this study to calculate the oxidation kinetic parameters,

#### Degree of conversion

Figure 4 shows the degree of conversion as a function of temperature at different heating rates (3–15  $^\circ\text{C min}^{-1}$ ). The degree of conversion was calculated from 100 to  $T_p$  that corresponded to the non-isothermal oxidation range of various edible fats and oils [23, 26, 27]. The curves for all AMF samples were sigmoid in shape regardless the heating rate. These curves represent reaction steps, occurring during non-isothermal oxidation, which can be individually described by the Arrhenius like model. For low heating rates, the oxidation event consists of several reactions having comparable effective activation energy values that slightly modify the general pattern of degree of conversion curves (Fig. 4a–c). Increasing the heating rate clearly modifies the general pattern of degree of conversion curves (lines 4 and 5). Two reasons could explain such a behavior: (i) reactions with high values of effective activation energy become more predominant than those reactions with low values of effective activation energy, and (ii) structural changes induced by the heating rate might affect the oxidation kinetic [25]. For the first reason, a simulation of the

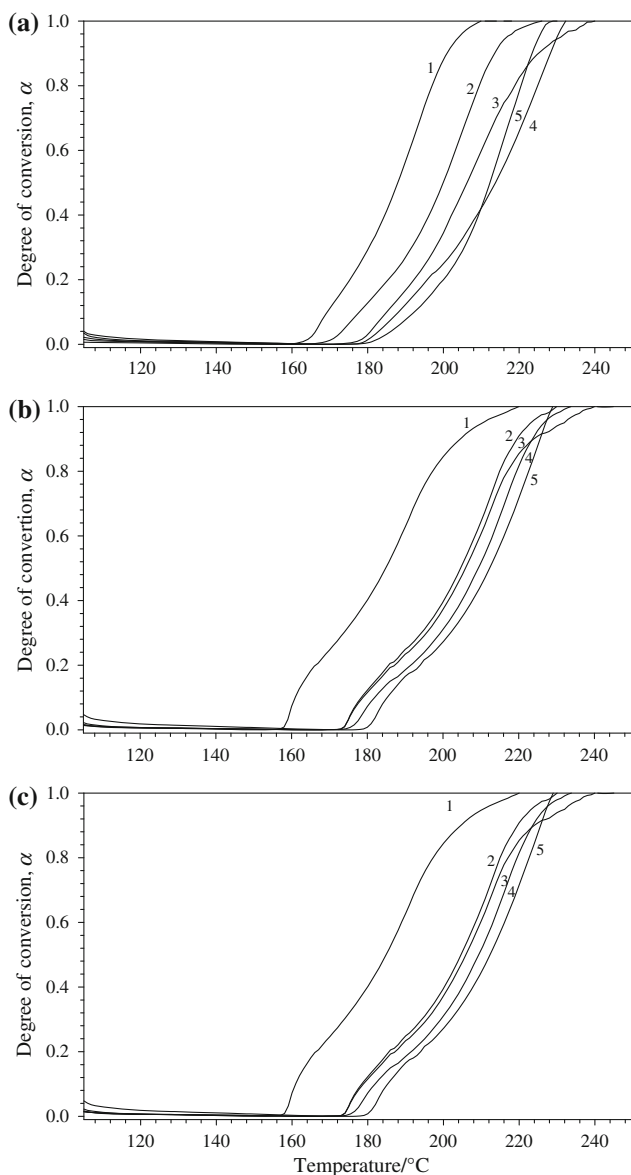


**Fig. 4** Degree of conversion as a function of temperature at different heating rates for: **a** L-CLA, **b** M-CLA, and **c** H-CLA. Line 1  $3\text{ }^{\circ}\text{C min}^{-1}$ , line 2  $6\text{ }^{\circ}\text{C min}^{-1}$ , line 3  $9\text{ }^{\circ}\text{C min}^{-1}$ , line 4  $12\text{ }^{\circ}\text{C min}^{-1}$ , and line 5  $15\text{ }^{\circ}\text{C min}^{-1}$

different reaction schemes is needed, which is beyond the scope of this article. The second reason is explored by the compensation effect.

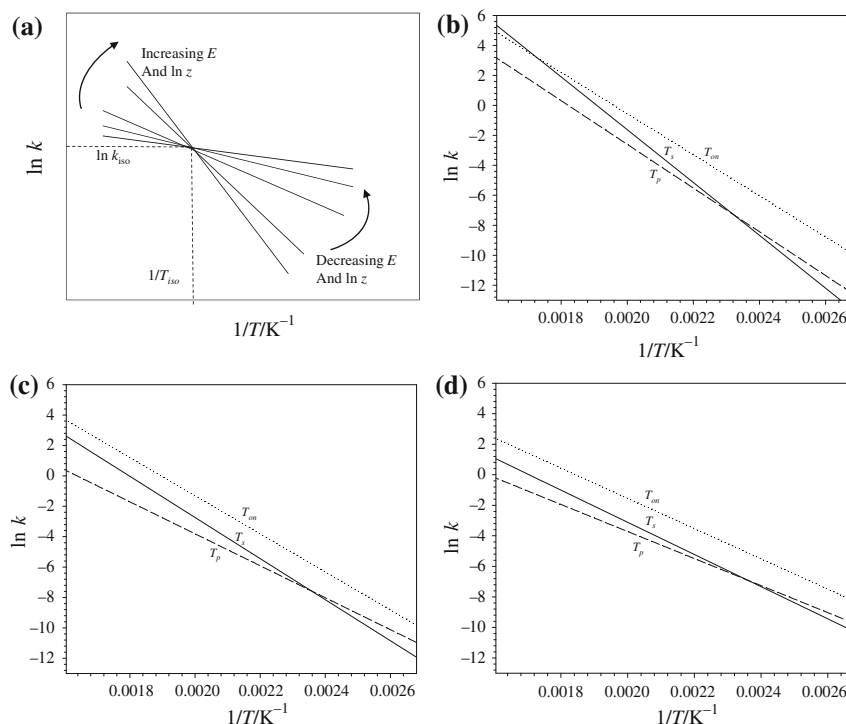
#### Compensation effect

Table 3 suggests that three major reactions occur during AMF oxidation having their own kinetic parameters. The different values of effective activation energy calculated

for AMF samples and therefore the oxidation rate associated with it strongly depends not only on the ratio between unsaturated to saturated fatty acids but also on the selected reference point ( $T_s$ ,  $T_{on}$ , and  $T_p$ ). Oxidation proceeds at different reaction rates. The reactions having low values of effective activation energy (Table 3) are favored at low heating rates and low temperatures (Table 2). These reactions occur over a broad temperature range (155–224 °C). Contrary, the reactions having high values of effective activation energy are promoted at high heating rates and high temperatures (Tables 2, 3), and the reaction temperature range increases [25, 27].

During non-isothermal oxidation, the reaction systems suffer modifications of thermophysical properties such as density, viscosity, etc., due to the linear increasing heating rate. Although structural modifications could change the kinetic parameters (effective activation energy and pre-exponential factor), these variations might not have physical background. A proper kinetic interpretation should include the compensation effect, which is usually used to explain whether the variations on effective activation energy values have physical meaning or they are caused by either variations of process conditions or complexity of the reaction systems. Agrawal [27, 28] compiled and illustrated the compensation effect of several thermal degraded materials (polymers, cellulosic materials, and  $\text{CaCO}_3$ ). The compensation effect (Fig. 5) can be evaluated by plotting  $\ln k$ , obtained by Eq. 5, against  $1/T$ . Figure 5a shows that an increase in the effective activation energy causes an increase in  $\ln z$  (Eq. 5). Similarly, a decrease in the effective activation energy results in a lower value of  $\ln z$ . The point of concurrence, where the different lines intercept, corresponds to  $\ln k_{iso}$  and  $1/T_{iso}$  ( $k_{iso}$  is the isokinetic rate constant and  $T_{iso}$  is the isokinetic temperature), which indicates the existence of compensation effect. In the case of AMF samples, there is no concurrence at a single point (Fig. 5b–d), meaning that the non-isothermal oxidation of AMF does not exhibit a compensation effect and therefore the variations in kinetic parameters (Table 2) do not have physical background. AMF is a very complex fat mainly composed by triacylglycerol that has a glycerol backbone to which three fatty acid moieties are esterified. These triacylglycerols are extremely diverse in chain lengths, position, and number of unsaturations of their fatty acids [30]. Moreover, Jensen [22] reported more than 400 fatty acids in milk fat. This diversity is reflected on the oxidative profiles (Figs. 3 and 4). Several reactions having different constant rates are simultaneously taking place and DSC only detects those reactions that have the greatest exothermal effect. This could explain why the variations in effective activation energy do not have physical meaning, according to the compensation theory.

**Fig. 5** Arrhenius plots ( $\ln k$  vs.  $1/T$ ) for the non-isothermal oxidation of anhydrous milk fat: **a** compensation effect (adapted from Agrawal [29]), **b** L-CLA, **c** M-CLA, and **d** H-CLA.  $E$  effective activation energy,  $\text{kJ mol}^{-1}$ ;  $z$  pre-exponential factor,  $\text{min}^{-1}$ ;  $T_{iso}$  and  $k_{iso}$  isokinetic rate constant and isokinetic temperature, respectively;  $T_s$ ,  $T_{on}$ , and  $T_p$  start, onset, and maximum temperatures of oxidation in K, respectively



## Conclusions

For the first time, non-isothermal oxidation of anhydrous milk fat rich in CLA was studied. This kinetic information can be used to predict and compare oxidative stability of AMF-based products. DSC is a fast and reliable method to evaluate the oxidation kinetics of AMF with different CLA compositions. The unsaturated fatty acid content shifts to low values of effective activation energy, while the content of saturated fatty acids increases the effective activation energy values. The shape of the DSC curves reveals the existence of different reactions that occur simultaneously but these variations do not have any physical background, according to the compensation theory. The start temperature of oxidation ( $T_s$ ) was the most consistent reference point in this study to calculate the kinetic oxidation parameters. Therefore, changes in  $T_s$  can be used to evaluate the oxidative profile of AMF rich in CLA.

**Acknowledgements** The authors thank to Alberta Livestock and Meat Agency Ltd. (ALMA) and Natural Sciences and Engineering Research Council of Canada-Collaborative Research and Development Grant (NSERC-CRD) for funding this project.

## References

- Velasco J, Andersen ML, Skibsted LH. Evaluation of oxidative stability of vegetable oils by monitoring the tendency to radical formation. A comparison of electron spin resonance spectroscopy with the rancimat method and differential scanning calorimetry. *Food Chem.* 2004;85(4):623–32.
- Simon P, Kolman L. DSC study of oxidation induction periods. *J Therm Anal.* 2001;64(2):813–20.
- Privett OS, Blank ML. Initial stages of autooxidation. *J Am Oil Chem Soc.* 1962;39(11):465–8.
- Adhvaryu A, Erhan SZ, Liu ZS, Perez JM. Oxidation kinetic studies of oils derived from unmodified and genetically modified vegetables using pressurized differential scanning calorimetry and nuclear magnetic resonance spectroscopy. *Thermochim Acta.* 2000;364(1–2):87–97.
- Kamal-Eldin A, Pokorny J. Lipid oxidation products and methods used for their analysis. In: Kamal-Eldin A, Pokorny J, editors. *Analysis of lipid oxidation*. Champaign: AOCS Publishing; 2005.
- Pokorny J. Volumetric analysis of oxidized lipids. In: Kamal-Eldin A, Pokorny J, editors. *Analysis of lipid oxidation*. Champaign: AOCS Publishing; 2005.
- Agrawal RK. Analysis of nonisothermal reaction-kinetics. I. Simple reactions. *Thermochim Acta.* 1992;203:93–110.
- Ozawa T. Critical investigation of methods for kinetic-analysis of thermoanalytical data. *J Therm Anal.* 1975;7(3):601–17.
- Thurgood J, Ward R, Martini S. Oxidation kinetics of soybean oil/anhydrous milk fat blends: a differential scanning calorimetry study. *Food Res Int.* 2007;40(8):1030–7.
- Litwinienko G. Autooxidation of unsaturated fatty acids and their esters. *J Therm Anal Calorim.* 2001;65(2):639–46.
- Litwinienko G, Daniluk A, Kasprzycka-Guttman T. Study on autooxidation kinetics of fats by differential scanning calorimetry. 1. Saturated C-12-C-18 fatty acids and their esters. *Ind Eng Chem Res.* 2000;39(1):7–12.
- Lock AL, Bauman DE. Modifying milk fat composition of dairy cows to enhance fatty acids beneficial to human health. *Lipids.* 2004;39(12):1197–206.
- Fritsche J, Rickert R, Steinhart H, Yurawecz MP, Mossoba MM, Sehat N, Roach JAG, Kramer JKG, Ku Y. Conjugated linoleic



- acid (CLA) isomers: formation, analysis, amounts in foods, and dietary intake. *Fett-Lipid*. 1999;101(8):272–6.
14. Cook ME, Pariza M. The role of conjugated linoleic acid (CLA) in health. *Int Dairy J*. 1998;8(5–6):459–62.
  15. Park Y. Conjugated linoleic acid (CLA): good or bad trans fat? *J Food Comp Anal*. 2009;22(Supplement 1):S4–12.
  16. Kennelly JJ, Bell JA. Increasing the concentration of conjugated linoleic acid isomers in the milk fat and/or tissue fat of ruminants. 2004; Application patent US 20030439501 20030516.
  17. Bell JA, Griinari JM, Kennelly JJ. Effect of safflower oil, flaxseed oil, monensin, and vitamin E on concentration of conjugated linoleic acid in bovine milk fat. *J Dairy Sci*. 2006;89(2):733–48.
  18. Walstra P, Wouters JTM, Geurts TJ. *Dairy science and technology*. 2nd ed. Boca Raton: CRC Taylor & Francis; 2006.
  19. Cruz-Hernandez C, Deng ZY, Zhou JQ, Hill AR, Yurawecz MP, Delmonte P, Mossoba MM, Dugan MER, Kramer JKG. Methods for analysis of conjugated linoleic acids and trans-18:1 isomers in dairy fats by using a combination of gas chromatography, silver-ion thin-layer chromatography/gas chromatography, and silver-ion liquid chromatography. *J AOAC Int*. 2004;87(2):545–62.
  20. Kramer JKG, Cruz-Hernandez C, Zhou JQ. Conjugated linoleic acids and octadecenoic acids: analysis by GC. *Eur J Lipid Sci Tech*. 2001;103(9):600–9.
  21. Bouzidi L, Boodhoo M, Humphrey KL, Narine SS. Use of first and second derivatives to accurately determine key parameters of DSC thermographs in lipid crystallization studies. *Thermochim Acta*. 2005;439(1–2):94–102.
  22. Jensen RG. The composition of bovine milk lipids: January 1995 to December 2000. *J Dairy Sci*. 2002;85(2):295–300.
  23. Ulkowski M, Musialik M, Litwinienko G. Use of differential scanning calorimetry to study lipid oxidation. 1. Oxidative stability of lecithin and linolenic acid. *J Agric Food Chem*. 2005;53(23):9073–7.
  24. Litwinienko G, Daniluk A, Kasprzycka-Guttman T. A differential scanning calorimetry study on the oxidation of C-12-C-18 saturated fatty acids and their esters. *J Am Oil Chem Soc*. 1999; 76(6):655–7.
  25. Litwinienko G, Kasprzycka-Guttman T. Oxidation of saturated fatty acids esters—DSC investigations. *J Therm Anal and Calorim*. 1998;54(1):211–7.
  26. Musialik M, Litwinienko G. DSC study of linolenic acid autoxidation inhibited by BHT, dehydrozingerone and olivetol. *J Therm Anal Calorim*. 2007;88(3):781–5.
  27. Arain S, Sherazi STH, Bhanger MI, Talpur FN, Mahesar SA. Oxidative stability assessment of *Bauhinia Purpurea* seed oil in comparison to two conventional vegetable oils by differential scanning calorimetry and rancimat methods. *Thermochim Acta*. 2009;484(1–2):1–3.
  28. Agrawal RK. The compensation effect—a fact or a fiction. *J Therm Anal*. 1989;35(3):909–17.
  29. Agrawal RK. On the compensation effect. *J Therm Anal*. 1986;31(1):73–86.
  30. Lopez C, Lavigne F, Lesieur P, Bourgaux C, Ollivon M. Thermal and structural behavior of milk fat. 1. Unstable species of anhydrous milk fat. *J Dairy Sci*. 2001;84(4):756–66.